

Temperature mapping in Human Brown Adipose Tissue Using Fat-Water MRI with Explicit Fitting of Water Peak Location

Aliya Gifford^{1,2}, Theodore F Towse^{1,3}, Malcolm J Avison^{1,4}, and E Brian Welch^{1,5}

¹Institute of Imaging Science, Vanderbilt University, Nashville, TN, United States, ²Chemical and Physical Biology Program, Vanderbilt University, Nashville, TN, United States, ³Department of Physical Medicine and Rehabilitation, Vanderbilt University, Nashville, TN, United States, ⁴Department of Pharmacology, Vanderbilt University, Nashville, TN, United States, ⁵Department of Radiology & Radiological Sciences, Vanderbilt University, Nashville, TN, United States

Purpose and Motivation: The current standard method for distinguishing activated and non-activated brown adipose tissue (BAT) employs ¹⁸F-Fluorodeoxyglucose (¹⁸F-FDG) positron emission tomography (PET) and x-ray computed tomography (CT), which delivers an undesirable radiation dose. The purpose of this work is to apply a novel fat-water MRI (FWMRI) method with explicit modeling of temperature-dependent water frequency offset to scans of activated and non-activated BAT in adult human subjects to demonstrate the method's ability to distinguish between the BAT states.

Methods: The study was approved by the local ethics committee to recruit healthy adult subjects to undergo both FWMRI and PET-CT scans. Both FWMRI and PET-CT scans were performed twice, each scan on a separate day, once after two hours of exposure to cold-activating (CA) conditions (16°C (62°F)) and once after two hours of exposure to thermoneutral (TN) conditions (24°C (76°F)). Four subjects (3 males, 1 female, age range: 21.5 to 26.7 years, BMI range: 20.2 to 23.8) were scanned on a 3.0 Tesla Achieva MRI scanner (Philips Healthcare, Best, The Netherlands), equipped with two-channel parallel transmit capability, a 16-channel Torso-XL surface coil and an X-tend tabletop (X-tend ApS, Hornslet, Denmark). Multi-slice mFFE FWMRI scans were acquired at the clavicular level using both high and low spatial resolutions (HR and LR respectively). Scanner software was modified to enable the acquisition of interleaved sets of echoes, which reduces the effective TE without sacrificing scan resolution. Scan acquisition details are listed in **Table 1**. Three-dimensional water/fat separation and R2* estimation based on a multi-scale whole-image optimization algorithm¹ implemented in C++ was performed for each individual slice stack using a 9-peak fat model². The first echo of each 4-echo train was discarded to avoid potential contamination by eddy currents. Conventional fat/water separation results initialized a modified version of the mixed signal fitting algorithm available in the ISMRM Fat Water Toolbox³ based on the work⁴ of Hernando et al. The signal fitting function was modified to additionally solve for a temperature-dependent frequency shift of the water peak. PET-CT images were acquired on a GE Discovery STE PET/CT scanner (General Electric Medical Systems, Milwaukee, WI, USA) covering the same anatomy, with an acquired voxel size of 5.47 mm x 5.47 mm x 3.27 mm, and 1.36 mm x 1.36 mm x 3.27 mm respectively.

Results: Following the cold exposure, BAT activation was observed on the PET-CT scans for all but one subject, S11. It was later determined that this subject was taking a selective serotonin reuptake inhibitor, known to inhibit the activation of BAT. The other three subjects fell into two categories, S05 and S08 were normal activators, whose BAT activated during the CA scan, but not during the TN scan, while S07 was a “super-activator” whose BAT activated on both TN and CA scans. This PET standardized uptake values (SUV) uptake can be seen in **Figure 1**, column 4. To determine the regions of activated BAT the four imaging sessions were first coregistered for each subject, and then the CT Hounsfield units (HU) and PET SUV were used to define a BAT region of interest (ROI) without manual input. The following rules were used for automated generation of the BAT ROI: CT HU values: [-200 to -1], cold-activated PET > 2.0 SUV, and the ratio of cold-activated PET SUV to thermoneutral PET SUV > 0.5. The BAT ROI was refined by requiring that more than 15 immediately neighboring pixels (in 3D) must be part of the initial rule-based ROI. This ROI was used to select the region in the temperature map to analyze. **Figure 1** shows the results from one axial slice for each subject. Column 2 shows the fat-signal fraction map of the BAT ROI, with the corresponding masked temperature maps shown in column 3. The estimated average temperature offsets for each subject are listed in **Table 2**. The temperature offset measured with the HR mFFE scans was able to capture the temperature increase in all three activating subjects, S05, S08, and S07. The temperature for both normal activators during the warm scan was only slightly altered from normal body temperature, whereas the temperature offset was still increased in the “super-activator”, S07. BAT temperature for the non-activator, S11, was only slightly altered from normal body temperature during both the cold and warm scan. **Figure 1**, column 1, shows the histogram distribution of the HR scan estimate of temperature offset (°C) from body temperature, in the BAT ROI, shown in **Fig. 1**, column 3. The mean ± 95% C.I. of these histograms is listed in **Table 2**. The LR scan appears unreliable for measuring temperature offset in BAT possibly due in part to fewer echoes and/or larger voxel size.

Discussion and Conclusions: Despite the small number of subjects, this study demonstrates the possibility to distinguish activated from non-activated BAT in adult humans using FWMRI-derived temperature mapping. The elevated temperature in activated BAT is detectable in FWMRI scans following cold exposure compared to scans following warm conditions. To the best of our knowledge, this work presents the first report using MRI to determine the relative temperature change in BAT in adult humans. The results of this study demonstrate the potential of MRI to detect the activation state of brown adipose tissue.

References: [1] Berglund J, et al. MRM 67(6):1684-93; 2012. [2] Hamilton G, et al. NMR Biomed 24:784-790; 2011. [3] Hernando D, et al. ISMRM Fat Water Toolbox v1.0. <http://ismrm.org/workshops/FatWater12/data.htm> 2012 [4] Hernando D, et al. MRM 67(3):638-44; 2012. **Funding:** 1R21DK096282 from NIDDK/NIH & UL1 TR000445 from NCATS/NIH

	Low-Resolution	High-Resolution
TR/TE1/ΔTE (ms)	83 / 1.024 / 0.779	420 / 1.418 / 0.7833
Echo count	4 x 2 interleaves	4 x 3 interleaves
α (°)	12	30
(Act.) Water Fat Shift	0.323 pixels	0.452 pixels
Readout Band Width	1346.1 Hz/pixel	961.5 Hz/pixel
Sensitivity Encoding	3	1.5
Axial field-of-view (mm)	520 x 408	520 x 408
Acq. Voxel size (mm)	2 x 2 x 7.5	1 x 1 x 5
Slices / slice gap (mm)	20 / 0	30 / 0

Table 1: Low- and high-resolution FWMRI scan parameters.

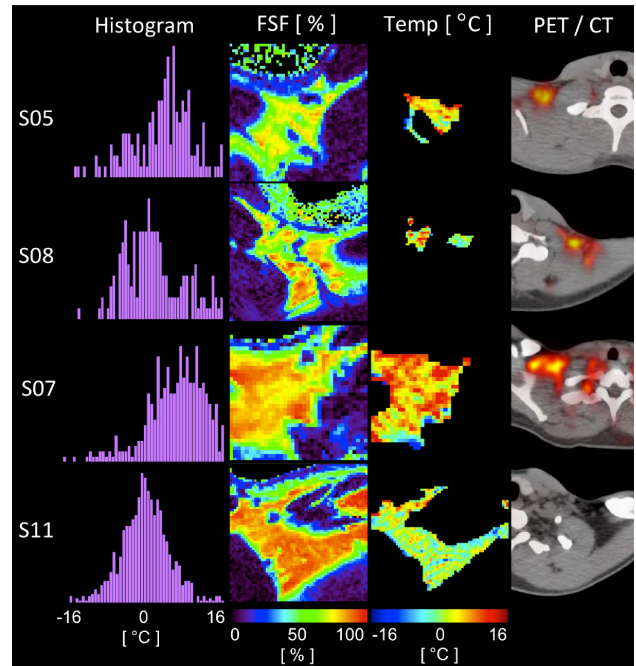


Figure 1 - Axial slices from high-resolution mFFE cold-activation scans showing: column 1: histograms of temperature, column 2: FSF maps, column 3: masked temperature maps, column 4: PET activation on CT.

	PET	CA HR	TN HR	CA LR	TN LR
S05	+	[†] 3.7 ± 0.9	* 1.2 ± 0.7	-0.7 ± 0.9	-4.8 ± 0.9
S08	+	[†] 2.1 ± 0.8	-1.6 ± 0.5	-5.3 ± 1.0	-5.4 ± 0.8
S07	+	[†] 6.2 ± 0.6	[†] 4.1 ± 0.7	5.4 ± 0.5	1.9 ± 0.7
S11	-	* 0.6 ± 0.3	-0.4 ± 0.3	-6.2 ± 0.3	-9.0 ± 0.4

Table 2. Temperature offset (°C) mean ± 95% C.I. in the BAT ROI from both cold (CA) and warm (TN) high- and low-resolution scans. The PET column indicates PET confirmed BAT: ‘+’: BAT positive, ‘-’: BAT negative. Right-tail t-test of the CA HR data shows the mean is significantly greater than zero for all subjects. Right-tail t-test of the TN HR data shows only S05 and S07 are significantly greater than zero. (* p < 0.001, [†] p < 1e-6).